# Extended projector method: Application to Jahn-Teller and pseudo-Jahn-Teller systems

Marc Vanhimbeeck, Hans De Raedt, and Dirk Schoemaker

*Department of Physics, University of Antwerp, Universiteitsplein 1, B-2610 Wilrijk, Belgium*

(Received 11 January 1988)

Within the Trotter-Suzuki approximations on $e^{-\beta H}$, the extended projector method [Phys. Rev. A **36**, 4612 (1987)] previously introduced by us is shown to be a valuable technique in investigating the general class of few-level systems coupled both linearly and quadratically to a selected number of harmonic oscillators. As an illustration we compare eigenvalues and Ham-reduction factors with the literature for the cubic linear Jahn-Teller systems $T \otimes \epsilon$ and $T \otimes \tau_2$ as well as for the system $E \otimes \epsilon$ for which a quadratic warping interaction is included. For the latter system a symmetry projector is additionally developed, dealing with the transformation properties of nonlinear combinations of representational basis functions. As another illustration, the low-energy eigenstates of a two-level system quadratically coupled to a single harmonic oscillator are investigated. Within the ground state, the system becomes unstable at high coupling strengths and through the evaluation of time- and frequency-dependent correlation functions we found substantially different ground-state dynamic properties compared with those of a linearly coupled system.

## I. INTRODUCTION

We propose a numerical treatment of a general quantum-mechanical few-level system coupled to a finite set of harmonic oscillators. Such a model is frequently applied as a nontrivial description of complex physical systems. The few-level approximation is generally based on the idea that only a selected set of states of the system is to be considered as relevant for the physical process under study. Well-known examples are spin-resonance theory and optical transition models in which some external resonance conditions (e.g., microwaves, incident laserlight) and general level-occupation considerations (e.g., thermal equilibrium distribution or nonequilibrium initial-state preparation) justify the simplification of the few-level approximation for the complex electronic structures. Another class of systems in which one is naturally led to employ the few-level description is the Jahn-Teller (JT) and pseudo-Jahn-Teller (PJT) systems in molecular and solid-state physics, the few-level system being defined by degenerate (JT) or nearly degenerate (PJT) electronic multiplets. Of a nonelectronic nature are problems involving tunneling and reorientation between a finite number of spatially distinct states which are most adequately described with a few-level model, associating each "level" with a possible spatial configuration. In solid-state physics the coupling to harmonic oscillators often describes the interaction of the few-level system, embedded in a crystalline host, with the lattice vibrations. We already mentioned the JT systems, but other examples include spin-lattice relaxation theory,[1] the molecular polaron,[2-6] phonon-assisted tunneling,[3,7-9] and the theory of radiationless transitions.[10,11] It should immediately be noted that we will not treat a continuous bath of phonons, but only allow for a finite number of oscillators. They are associated with the "effective" lattice deformations and are often expressed in terms of the normal modes of a cluster consisting of the few-level system surrounded by a small number of lattice ions.[12] We finally mention quantum optics in which this kind of coupling to harmonic oscillators is used to model the interaction of the few-level system with a radiation field.[13]

The plan of the paper is as follows. In Sec. II we present the generic Hamiltonian and propose a way in which it can be suited for an application of the extended projector method (EPM). As a first example, a two-level system with quadratic coupling to a single harmonic oscillator is treated in Sec. III. This system can be considered as a simple PJT system. A similar treatment of the corresponding linearly coupled model has been given earlier.[14] Section IV is devoted to the cubic JT systems $T \otimes \epsilon$ and $T \otimes \tau_2$ for which only a linear interaction term is considered, as well as to the system $E \otimes \epsilon$, which is treated with the inclusion of a quadratic JT warping term. Whereas the bare EPM is applied for the systems $T \otimes \epsilon$ and $T \otimes \tau_2$, a further refinement, exploiting the symmetry properties at maximum, is worked out for $E \otimes \epsilon$.

## II. GENERAL THEORY

The general Hamiltonian that we will consider reads as follows ($\hbar = 1$):

$$\mathcal{H} = \mathcal{H}_L + \mathcal{H}_{OO} + \sum_{i=1}^{\gamma} \mathcal{H}_{LO}^{(\Gamma)}(i) + \sum_{i,j=1}^{\gamma} \mathcal{H}_{LOO}^{(\Gamma')}(i,j) , \quad (2.1a)$$

with

$$\mathcal{H}_L = hL , \quad (2.1b)$$

$$\mathcal{H}_{OO} = \Omega \sum_{i=1}^{\gamma} a_i^{\dagger} a_i , \quad (2.1c)$$

$$\mathcal{H}_{LO}^{(\Gamma)}(i) = (\Omega C_1)^{1/2} L_i^{(\Gamma)} (a_i^{\dagger} + a_i) , \quad (2.1d)$$

$$\mathcal{H}_{LOO}^{(\Gamma')}(i,j) = \Omega C_2 \sum_{k=1}^{\gamma'} L_k^{(\Gamma')} f_k^{(\Gamma')}(i,j)(a_i^{\dagger} + a_i)(a_j^{\dagger} + a_j) . \quad (2.1e)$$

$\mathcal{H}_L$ represents the Hamiltonian of the few-level system, henceforth assumed to be of dimension $l$ and is described in terms of an $(l \times l)$ matrix $L$, transforming in a totally symmetric way under the elements of the system's symmetry group $\mathcal{G}$. By definition, the oscillator coordinates can be chosen as to transform according to an irreducible representation $\Gamma$ (dimension $\gamma$) of $\mathcal{G}$ and are labeled with respect to the different rows of this representation (indices $i,j$). $\mathcal{H}_{OO}$ models the free oscillators, all assumed to have the same frequency $\Omega$, in terms of the creation (annihilation) operator $a_i^\dagger$ ($a_i$) for oscillator $i$. By application of Unsöld's theorem,[15] the linear coupling term $\mathcal{H}_{LO}^{(\Gamma)}$ (sum over all $i$) is totally symmetric if the $(l \times l)$ matrix $L_i^{(\Gamma)}$ transforms, just as the $i$th oscillator coordinate $(a_i^\dagger + a_i)$, according to the $i$th row of $\Gamma$. $C_1$ describes the linear coupling strength which is, in the absence of quadratic coupling, proportional to the binding energy of the displaced oscillators, the proportionality depending on the normalization-convention of $L_i^{(\Gamma)}$. The quadratic coupling term $\mathcal{H}_{LOO}^{(\Gamma')}(i,j)$ is somewhat more subtle, as one now has to combine an $(l \times l)$ matrix $L_k^{(\Gamma')}$, transforming according to the $k$th row of a representation $\Gamma'$ (dimension $\gamma'$ and $\Gamma'$ not necessarily equal to $\gamma$ and $\Gamma$), with a suitable linear combination of quadratic forms of the oscillator-coordinates belonging to $\Gamma$. Knowing, by definition, the transformation properties of these oscillator coordinates the proper coefficients $f_k^{(\Gamma')}(i,j)$ can be found from group theory by constructing a quadratic form, transforming as the $k$th row of representation $\Gamma'$. In this way, $\mathcal{H}_{LOO}^{(\Gamma')}$ (sum over $i,j$) is again assured to transform in a totally symmetric way. $C_2$ is the quadratic coupling strength which, in contrast with $C_1$, will not displace the oscillators, but rather modulate their frequency. As the frequency is to remain positive, the modulation depth is limited and $C_2$ is bounded from above, the exact limits depending on the normalization conventions applied for $L_k^{(\Gamma')}$ and $f_k^{(\Gamma')}$. An example of this limit will be studied in Sec. III A. Note that we have implicitly assumed to couple quadratically twice to oscillators of the same representation $\Gamma$, which necessarily implies $\Gamma' \in \Gamma \times \Gamma$. This of course is not strictly required and one can equally well couple quadratically to two kinds of oscillators belonging to different representations. As this only makes the notation more cumbersome this case has not been incorporated in (2.1).

Taking as basis states a truncated set of oscillator eigenstates $|0_i\rangle, |1_i\rangle, \ldots, |N_i\rangle$ (i.e., $a_i^\dagger a_i |n_i\rangle = n_i |n_i\rangle$, $0 \le n_i \le N_i$) for each oscillator $i = 1, 2, \ldots, \gamma$, Hamiltonian (2.1) will be represented in the direct product space of all such oscillator states with the $l$ few-level states. In general, the total dimension $l \prod_{j=1}^{\gamma} N_j$ can easily exceed the limit up to which matrices can be handled with numerical diagonalization techniques. It has, however, been shown[14] that low-energy eigenstates as well as their dynamics can still be evaluated numerically for such systems within the formalism of the Trotter-Suzuki[16-20] approximation. The operator $e^{-\beta \mathcal{H}}$ can be considered as a projector onto the low-energy eigenstates of $\mathcal{H}$ for $\beta$ sufficiently large. A combination of the projector on a finite collection of states, say, $d$ in number, with the vari-

ational principle, has been worked out such that the set of projected states can be shown to span the subspace of the $d$ lowest-energy eigenstates of $\mathcal{H}$, no matter the (quasi)degeneracies within this subspace. The general technique, from now on to be referred to as extended projector method, is explained in detail in Ref. 14, where it is applied to a two-level system linearly coupled to a single harmonic oscillator. Whereas approximations on $e^{-\beta \mathcal{H}}$ are important in order to find a low-energy eigenstate $|\Psi\rangle$ of $\mathcal{H}$, similar approximations on $e^{-it\mathcal{H}}$ allow the calculation of its time dependence ($|\Psi(t)\rangle = e^{-it\mathcal{H}}|\Psi\rangle$), as well as of time-dependent correlation functions such as $\langle O(t)O(0)\rangle \equiv \langle \Psi | e^{it\mathcal{H}} O e^{-it\mathcal{H}} O | \Psi\rangle$ for any operator $O$.[14] Following Ref. 14 this work will exclusively deal with the following symmetrized approximation on $e^{-bH}$ ($\beta = mb$) (Refs. 16 and 17):

$$e^{-bH(b)} \equiv e^{-bH_A/2} e^{-bH_B} e^{-bH_A/2} , \tag{2.2a}$$

for an arbitrary separation of $H = H_A + H_B$ and correct to second order in $b$

$$\|e^{-mbH} - (e^{-bH(b)})^m\| \le \mathcal{O}(mb^3) , \tag{2.2b}$$

equally valid for $b = i\tau$. A detailed analysis of second-order product formulas such as (2.2), as well as of fourth-order extensions, is given elsewhere.[21] Formula (2.2) is readily generalized to a separation of $H$ in any number of parts. One typically keeps splitting the Hamiltonian into smaller pieces until the final parts can be exponentiated easily. In the remainder of this section, we will discuss in some detail the splitting-scheme that we employed on Hamiltonian (2.1).

Since the few-level system is essentially assumed to be of a relatively low dimension, all $(l \times l)$ matrices will be treated numerically exact through the use of diagonalization procedures. The block-diagonal matrices $\mathcal{H}_L$ and $\mathcal{H}_{OO}$ can be exponentiated by numerically exact calculations. The further discussion of (2.1) is therefore essentially a discussion of the oscillator problem of dimension $N^{(\gamma)} \equiv \prod_{j=1}^{\gamma} N_j$, keeping in mind that each entity in this problem is in fact an $(l \times l)$ matrix. We propose

$$e^{-b\mathcal{H}(b)} \equiv e^{-b(\mathcal{H}_L + \mathcal{H}_{OO})/2}$$

$$\times \left[ \prod_{i=1}^{\gamma} e^{-b\mathcal{H}_{LO}^{(\Gamma)}(i)/2} \right] \left[ \prod_{i,j=1}^{\gamma} e^{-b\mathcal{H}_{LOO}^{(\Gamma')}(i,j)} \right]$$

$$\times \left[ \prod_{i=1}^{\gamma} e^{-b\mathcal{H}_{LO}^{(\Gamma)}(i)/2} \right] e^{-b(\mathcal{H}_L + \mathcal{H}_{OO})/2} , \tag{2.3}$$

where we have factorized commuting oscillators. To treat the remaining coupling Hamiltonians $\mathcal{H}_{LO}^{(\Gamma)}(i)$ and $\mathcal{H}_{LOO}^{(\Gamma')}(i,j)$ we will, for notational convenience, reformulate them in a fermion formalism[21] which is fully equivalent with the matrix representation in the $N^{(\gamma)}$-dimensional basis. Considering oscillator $i$, we introduce the creation operator $c_{n_i}^\dagger$ of the occupational state $|n_i\rangle \equiv c_{n_i}^\dagger |0_i\rangle$. Within the previously made truncation approximation of a finite oscillator representation $\sum_{i=1}^{N_i} |n_i\rangle\langle n_i| = 1 = \sum_{i=1}^{N_i} c_{n_i}^\dagger c_{n_i}$, one can easily check

that

$$\mathcal{H}_{LO}^{(\Gamma)}(i)=L_i^{(\Gamma)}\tilde{\mathcal{H}}_{LO}^{(\Gamma)}(i) ,  \qquad (2.4a)$$

$$\tilde{\mathcal{H}}_{LO}^{(\Gamma)}(i)=(\Omega C_1)^{1/2}(a_i^\dagger+a_i) ,  \qquad (2.4b)$$

$$\tilde{\mathcal{H}}_{LO}^{(\Gamma)}=(\Omega C_1)^{1/2}\sum_{i=0}^{N_i-1}(n_i+1)^{1/2}(c_{n_i}^\dagger c_{n_i+1}+c_{n_i+1}^\dagger c_{n_i}) ,$$

$$(2.4c)$$

and

$$\mathcal{H}_{LOO}^{(\Gamma)}(i,j)=\sum_{k=1}^{\gamma'}L_k^{(\Gamma')}\tilde{\mathcal{H}}_{LOO}^{(\Gamma')}(i,j;k) ,  \qquad (2.5a)$$

$$\tilde{\mathcal{H}}_{LOO}^{(\Gamma')}(i,j;k)=\Omega C_2 f_k^{(\Gamma')}(i,j)(a_i^\dagger+a_i)(a_j^\dagger+a_j) ,  \qquad (2.5b)$$

$$\tilde{\mathcal{H}}_{LOO}^{(\Gamma')}(i,j;k)=\begin{cases}\Omega C_2 f_k^{(\Gamma')}(i,j)\left[\sum_{n_i=0}^{N_i-1}(n_i+1)^{1/2}(c_{n_i}^\dagger c_{n_i+1}+c_{n_i+1}^\dagger c_{n_i})\right]\left[\sum_{n_j=0}^{N_j-1}(n_j+1)^{1/2}(c_{n_j}^\dagger c_{n_j+1}+c_{n_j+1}^\dagger c_{n_j})\right] ,  & i\neq j \\[4mm] \Omega C_2 f_k^{(\Gamma')}(i,i)\left[\sum_{i=0}^{N_i-2}[(n_i+2)(n_i+1)]^{1/2}(c_{n_i}^\dagger c_{n_i+2}+c_{n_i+2}^\dagger c_{n_i}) , +\sum_{i=0}^{N_i}(2n_i+1)c_{n_i}^\dagger c_{n_i}\right], & i=j .\end{cases}$$

$$(2.5c)$$

The linear coupling (2.4c) is interpreted as a nearest-neighbor interaction on the one-dimensional chain of oscillator states. For the quadratic coupling (2.5c) one distinguishes the cases of nearest-neighbor hopping on a two-dimensional lattice for the coupling with two distinct oscillators $(i\neq j)$ and the next-nearest-neighbor hopping, complemented with a self-interaction for the quadratic coupling with only one oscillator $(i=j)$. The different coupling schemes are visualized in Fig. 1, together with the ultimate breakups that we now discuss.

For the linear coupling $\tilde{\mathcal{H}}_{LO}(i)$ we use a splitup, based on the even and odd sublattices, as depicted in Fig. 1(a) (Ref. 22)

$$e^{-b\tilde{\mathcal{H}}_{LO}(i)}\simeq e^{-b\tilde{\mathcal{H}}_{LO}^{(1)}(i)/2}e^{-b\tilde{\mathcal{H}}_{LO}^{(2)}(i)}e^{-b\tilde{\mathcal{H}}_{LO}^{(1)}(i)/2} ,  \qquad (2.6)$$

denoting the even and odd interactions with the indices 1 and 2, respectively, and having suppressed the represen-

tation index $(\Gamma)$. Since each interaction in the right-hand side of Eq. (2.6) consists of a set of commuting two-site interactions [see Fig. 1(a)], the exponentiations in (2.6) break up into a lot of $(2\times2)$ problems, one corresponding to each such pair of sites. Recalling that the $(2\times2)$ problem is built from matrices, proportional to $L_i^{(\Gamma)}$, each exponentiation involves a $(2l\times2l)$ matrix and has to be solved numerically. The quadratic coupling $\mathcal{H}_{LOO}(i,j)$ [Fig. 1(b)] is the two-dimensional analog of $\tilde{\mathcal{H}}_{LO}(i)$ and is broken up as follows:

$$e^{-b\tilde{\mathcal{H}}_{LOO}(i,j)}\simeq e^{-b\tilde{\mathcal{H}}_{LOO}^{(1)}(i,j)/2}e^{-b\tilde{\mathcal{H}}_{LOO}^{(2)}(i,j)/2}$$
$$\times e^{-b\tilde{\mathcal{H}}_{LOO}^{(3)}(i,j)/2}e^{-b\tilde{\mathcal{H}}_{LOO}^{(4)}(i,j)}$$
$$\times e^{-b\tilde{\mathcal{H}}_{LOO}^{(3)}(i,j)/2}e^{-b\tilde{\mathcal{H}}_{LOO}^{(2)}(i,j)/2}$$
$$\times e^{-b\tilde{\mathcal{H}}_{LOO}^{(1)}(i,j)/2} .  \qquad (2.7)$$
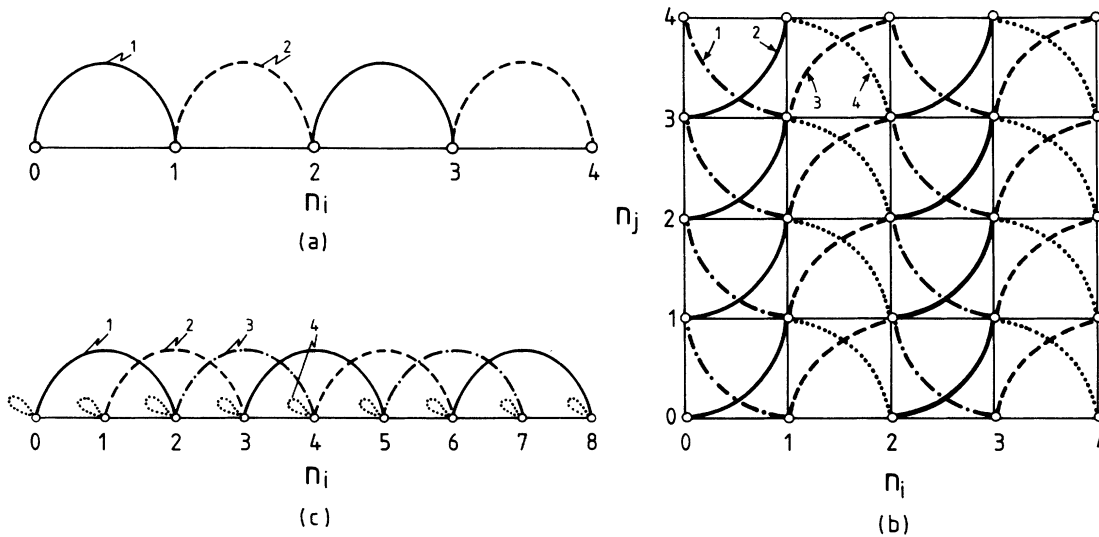


FIG. 1. Visualization of the splitting schemes applied in the symmetrized product approximations on the various parts of the Hamiltonian. Part (a) shows the even-odd separation for a simple one-dimensional lattice as it appears in the treatment of the linear interaction term $\tilde{\mathcal{H}}_{LO}(i)$, with (b) an equivalent extension to two dimensions for the analysis of its quadratic counterpart $\tilde{\mathcal{H}}_{LOO}(i,j)$. Finally, the three next-nearest-neighbor interactions and the self-interaction of $\tilde{\mathcal{H}}_{LOO}(i,i)$ are shown in part (c).

Finally, $\tilde{\mathcal{H}}_{LOO}(i,i)$ is split into three commuting pair interactions (1,2,3) and one self-interaction term (4) [Fig. 1(c)], leading to

$$e^{-b\tilde{\mathcal{H}}_{LOO}(i,i)} \simeq e^{-b\tilde{\mathcal{H}}_{LOO}^{(1)}(i,i)/2} e^{-b\tilde{\mathcal{H}}_{LOO}^{(2)}(i,i)/2}$$

$$\times e^{-b\tilde{\mathcal{H}}_{LOO}^{(3)}(i,i)/2} e^{-b\tilde{\mathcal{H}}_{LOO}^{(4)}(i,i)}$$

$$\times e^{-b\tilde{\mathcal{H}}_{LOO}^{(3)}(i,i)/2} e^{-b\tilde{\mathcal{H}}_{LOO}^{(2)}(i,i)/2}$$

$$\times e^{-b\tilde{\mathcal{H}}_{LOO}^{(1)}(i,i)/2} . \tag{2.8}$$

Summarizing, we have indicated in this section how, within the context of the Trotter-Suzuki approximation, exponents of the most general Hamiltonian of a few-level system, coupled both linearly and quadratically to a finite collection of harmonic oscillators can be split into commuting pair interactions. In this scheme the operation therefore reduces to an exponentiation of $(2l \times 2l)$ matrices, whereby $l$ denotes the dimension of the few-level system.

## III. PSEUDO-JAHN-TELLER SYSTEMS

The Hamiltonians to be studied in this section model two-level systems, quadratically coupled to a single harmonic oscillator. Such a second-order coupling is not very common and, indeed, similar systems with linear coupling are more frequently applied in, e.g., solid-state physics. As we did, however, already treat the linear-coupling problem with the EPM previously[14] the case of quadratic coupling is presented here as an evident extension. It will be shown that the physics of the latter differ substantially from that of the former case. First we will study some of the static ground-state properties of these systems in connection with a possible transition as a function of the coupling strength. Then, the ground-state dynamics will be investigated through the evaluation of some representative time-correlation functions.

### A. Statics

The Hamiltonian $(\hbar = 1)$ under consideration reads

$$\mathcal{H} = \mathcal{H}_L + \mathcal{H}_{OO} + \mathcal{H}_{LOO} , \tag{3.1a}$$

with

$$\mathcal{H}_L = -h\sigma^z , \tag{3.1b}$$

$$\mathcal{H}_{OO} = \Omega a^\dagger a , \tag{3.1c}$$

$$\mathcal{H}_{LOO} = \frac{C_2\Omega}{4}(a^\dagger + a)^2\sigma^x . \tag{3.1d}$$

$\sigma^x$ and $\sigma^z$ are Pauli spin-$\frac{1}{2}$ operators describing a two-level system with frequency $2h$. It is quadratically coupled through $\mathcal{H}_{LOO}$ to a harmonic-oscillator mode with frequency $\Omega$, $C_2$ determining the coupling-strength. Recently, model (3.1) has been studied in the adiabatic limit (neglect of the kinetic energy in $\mathcal{H}_{OO}$) at finite temperatures[23] for this approximation allowed a comparison of the authors' numerical results based on a discrete path-integral representation of the partition function with the

exact thermodynamic properties which can be computed numerically to any precision. Especially the derivative of the free energy $F$ with respect to $C_2$ is of interest as a discontinuity in $\partial F/\partial C_2$ or $\partial^2 F/\partial C_2^2$ as a function of $C_2$ reveals a transition in the ground state.

In this section we extend the results of Ref. 23 by calculating zero-temperature properties without relying on the adiabatic-limit assumption. From (3.1) one finds in the zero-temperature limit

$$\frac{\partial E}{\partial C_2} = \frac{\Omega}{4}\langle \Psi_0 | \sigma^x(a^\dagger + a)^2 | \Psi_0 \rangle , \tag{3.2}$$

where the ground state of $\mathcal{H}$ is denoted by $|\Psi_0\rangle$. We have performed a numerical diagonalization of the truncated matrix considering oscillator states $|0\rangle \cdots |N\rangle$ with $N = 30$ and 60, rather than apply the EPM to determine $|\Psi_0\rangle$. The values of $-\partial E/\partial C_2$ are presented in Fig. 2 for various values of $h$ (units of $\Omega = 1$) and in the neighborhood of $C_2 = 1$.

It is instructive to start the discussion with the special case $h = 0$, for this considerable simplification allows an analytic solution of the problem. As the two eigenstates of $\sigma^x$ are now uncoupled, the problem is block diagonal with respect to the spin coordinates, each block representing a harmonic oscillator with modulated frequency $\Omega(1 \pm C_2)^{1/2}$ ($\pm$ for the respective blocks). Using the known ground state it is easily shown that

$$-\frac{\partial E}{\partial C_2} = \frac{\Omega}{4(1 - C_2)^{1/2}} . \tag{3.3}$$

Obviously $\partial E/\partial C_2$ diverges at $C_2 = 1$. Notice also that $\partial E/\partial C_2 \neq 0$ if $C_2 = 0$. In Fig. 2, the numerical truncation of the system causes the divergency to be cut off. A better approximation (i.e., steeper and closer to $C_2 = 1$) is
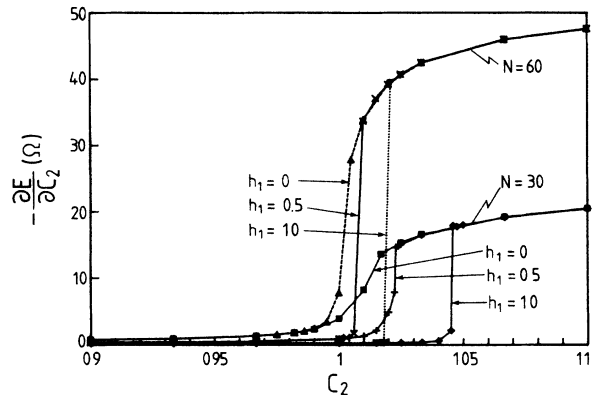


FIG. 2. Behavior of $-\partial E/\partial C_2$ as a function of the coupling constant $C_2$ for a two-level system quadratically coupled to a harmonic oscillator. The oscillator's mass $M$ and frequency $\Omega$ are taken as unity. The system's instability at $C_2 = 1$ is reflected by the finite jump near $C_2 \simeq 1$. The expected divergent behavior is recovered if the number of states $N$ used to represent the oscillator tends to infinity. The finite-$N$ effect is only important in the direct neighborhood of the critic coupling $C_2 = 1$, as can be seen from the collapsing of all lines for $C_2 < 0.99$. Also notice that for increasing tunneling frequency $2h$ the value of $-\partial E/\partial C_2$ decreases.

obtained for increasing $N$. Notice, however, that this is only critical near $C_2 = 1$. For smaller values of $C_2$, the two approximations $(N = 30,60)$ are undistinguishable and even in perfect agreement with (3.3), as can be seen from Table I. For $h \neq 0$ it is seen that $-\partial E / \partial C_2$ shows an overall decrease. The transition gets sharper but occurs at too high a value for $C_2$, shifting, however, closer to $C_2 = 1$ for increasing dimension $N$.

What should be retained from this section is that the number of oscillator states taken into account is only of critical importance in the neighborhood of the transition point $C_2 = 1$. As long as one stays away from this point, there is no need in making $N$ large.

## B. Dynamics

Here we will deal with Hamiltonian ($\hbar = 1$)

$$\mathcal{H} = \mathcal{H}_L + \mathcal{H}_{OO} + \mathcal{H}_{LOO} , \tag{3.4a}$$

with

$$\mathcal{H}_L = h\sigma^x , \tag{3.4b}$$

$$\mathcal{H}_{OO} = \Omega a^\dagger a , \tag{3.4c}$$

$$\mathcal{H}_{LOO} = \frac{C_2\Omega}{4}(a^\dagger + a)^2\sigma^x , \tag{3.4d}$$

which is very similar to (3.1) except for $\mathcal{H}_L$ which is now of the same nature as the tunneling part in $\mathcal{H}_{LOO}$. This additional simplification makes the model extremely simple as one now has, in much the same way as with the $h = 0$ case discussed in connection with (3.1), a problem which is block diagonal in the spin coordinates. The eigenvalues of (3.4) are given by

$$E_\pm(n_\pm) = (n_\pm + 1/2)\Omega\sqrt{1\pm C_2} \pm h - 1/2\Omega , \tag{3.5}$$

where the $\pm$ sign corresponds to the eigenvalues of $\sigma^x$. Within each subspace ($\pm$) one finds the spectrum of a modulated harmonic oscillator [frequency $\Omega(1\pm C_2)^{1/2}$] with the additional correction term $-1/2\Omega$ to account for the zero-point motion interaction. As the corresponding eigenstates $|n_\pm\pm\rangle$ of (3.5) can be expressed in terms of the modulated harmonic eigenfunctions, Hamiltonian (3.4) is exactly solvable.

We will now continue with a determination of the ground state $|\Psi_0\rangle$ through numerical diagonalization of

TABLE I. Values of $-\partial E / \partial C_2$ for system (3.1) with $h = 0$ and $\Omega = 1$ as a function of the coupling strength $C_2$, obtained from the exact result (3.3) (second column) and through numerical diagonalization of a $62\times 62$ (i.e., $N = 30$) matrix (third column). Notice also from Fig. 1 that the $N$ dependency is only significant near the transition coupling strength $C_2 = 1$.

| $C_2$ | $1/[4(1-C_2)^{1/2}]$ | $-(\partial E / \partial C_2)_{N=30}$ |
|---|---|---|
| 0.2 | 0.2795 | 0.2795 |
| 0.4 | 0.3228 | 0.3228 |
| 0.6 | 0.3953 | 0.3953 |
| 0.8 | 0.5590 | 0.5590 |
| 0.9 | 0.7906 | 0.7906 |
| 1.0 | $\infty$ | 3.98 |

a finite-dimensional matrix representation considering the oscillator states $|0\rangle \ldots |N\rangle$ with $N = 30$ which, we have checked, yields sufficiently accurate results for $0 \leq C_2 \leq 0.95$. With the knowledge of $|\Psi_0\rangle$ and using the Trotter-Suzuki approximations proposed in Sec. II for $b = i\tau$, imaginary, one can determine the zero-temperature time-correlation function of an operator $O$ from

$$\langle O(t)O(0)\rangle$$

$$\equiv \frac{\langle \Psi_0 | e^{it\mathcal{H}}Oe^{-it\mathcal{H}}O | \Psi_0\rangle - |\langle \Psi_0 | O | \Psi_0\rangle|^2}{\langle \Psi_0 | O^2 | \Psi_0\rangle - |\langle \Psi_0 | O | \Psi_0\rangle|^2} w(t) . \tag{3.6}$$

Notice that we have normalized to the $t = 0$ function value and subtracted the constant part $|\langle \Psi_0 | O | \Psi_0\rangle|^2$. For numerical convenience (3.6) is multiplied by a window-function $[w(t)]$ before calculating the structure factor $\mathcal{S}_{OO}(\omega)$, defined as the Fourier transform of the real part (Re) of the correlation function $\langle O(t)O(0)\rangle$

$$\mathcal{S}_{OO}(\omega) = -\frac{1}{2}\int_{-\infty}^{\infty} dt \, e^{i\omega t}\text{Re}(\langle O(t)O(0)\rangle) . \tag{3.7}$$

Due to the finite-dimensional representation, the spectral function $\mathcal{S}_{OO}(\omega)$ consists of $\delta$ functions at the ground-state transition frequencies of the operator $O$. As the $\delta$ functions imply, however, an infinite-length record of the correlation function $\langle O(t)O(0)\rangle$, a numerical Fourier transform at a finite record of length $T$ will result in overshootings near the transition frequencies (see, e.g., our previous linear coupling results[14]). It has been pointed out by Feit et al.[24] that this numerical problem can well be compensated for by choosing a proper window function $w(t)$ over the determined time interval $[0,T]$. These authors propose the Hanning window function

$$w(t) = \begin{cases} 1 - \cos(2\pi t/T) , & 0 \leq t \leq T \\ 0 , & t > T \end{cases} \tag{3.8}$$

but we found even better results (i.e., sharper frequency peaks) with

$$w(t) = \begin{cases} 1 + \cos(\pi t/T) , & 0 \leq t \leq T \\ 0 , & t > T \end{cases} \tag{3.9}$$

as (3.9), in contrast to (3.8), does preserve the short-time behavior of the correlation function. It should also be mentioned that equally good results were obtained with the Gaussian window function

$$w(t) = \begin{cases} e^{-\epsilon t^2} , & 0 \leq t \leq T \\ 0 , & t > t \end{cases} \tag{3.10}$$

provided its tails are sufficiently small, e.g., $e^{-\epsilon T^2} = 10^{-2}$.

In Figs. 3(a) and 3(c) we depict the time-dependent correlation functions of the operators $\sigma^z$ and $x = (2\Omega)^{-1/2}(a + a^\dagger)$ for system (3.4) with $h = 1$, $\Omega = 8$, and $C_2 = 0.9$, using the window function (3.9). The time propagator was approximated according to the general scheme of Sec. II with a value of $b = i\tau = i\pi/960$. The spectral functions $\mathcal{S}_{xx}$ and $\mathcal{S}_{\sigma\sigma}$, shown in Figs. 3(b) and 3(d) have been obtained from the time-dependent data by

using a 2048-point fast-Fourier transform. In the oscillator spectrum $\mathscr{S}_{xx}$ [Fig. 3(b)] of the operator $x$ the system's ground state $|0-\rangle$ can make a transition to the first excited vibrational state $|1-\rangle$ corresponding to the energy difference $\tilde{\Omega}=\Omega(1-C_2)^{1/2}$. The $C_2$ behavior can be checked from Fig. 4 where we plot the resonance frequencies $\tilde{\Omega}$ and $2\tilde{h}$ of $\mathscr{S}_{xx}$ and $\mathscr{S}_{\sigma\sigma}$, respectively, as a function of $C_2$, all other parameters $(\Omega,h,\tau,N)$ being constant. For $\sigma^z$ the state $|0-\rangle$ is expected to have nonzero matrix elements with all states of the form $|2m+\rangle$ $(m=0,1,2,3,\dots)$. The change of spin subspace is a consequence of the orthogonality relation between all oscillator states within one subspace ($|0-\rangle$ is a trivial exception contributing, however, at zero frequency and is therefore left out of consideration). Furthermore, the spatial inversion symmetry implies $|0-\rangle$ to make transitions only to even states $|2m+\rangle$. From (3.5) it follows that the resonance frequencies of $\mathscr{S}_{\sigma\sigma}$ [cf. Fig. 3(d)]

are given by

$$2\tilde{h}(m)=2h+(2m+1/2)\Omega(1+C_2)^{1/2}$$
$$-(\tfrac{1}{2})\Omega(1-C_2)^{1/2}\ , \quad m=0,1,2,3,\dots\ .$$

(3.11)

At $C_2=0$ one finds $2\tilde{h}(m)=2h+2m\,\Omega(C_2)^{1/2}$ but since at zero coupling only the bare tunneling frequency $2h$ can occur, one expects the intensities of all $m\neq0$ transitions to become negligibly small near $C_2=0$. This has indeed been observed from plots similar to Fig. 3(d) but made for smaller values of $C_2$. Consequently the $m\neq0$ lines in Fig. 4(b) could only be drawn for sufficiently high $C_2$. The presented data are in perfect agreement with (3.11).

## IV. JAHN-TELLER SYSTEMS

Characteristic for a JT system is the coupling of a degenerate electronic multiplet with some vibrational motion of either the embedding crystal or of the molecular ions constituting the complex. Well-known examples are the electronic doublet states $(E)$ in cubic symmetry which can couple to $E$ phonon modes (i.e., $E\otimes\epsilon$) and the triplet states $(T_1,T_2)$ coupled to $E$ or $T_2$ modes (i.e., $T\otimes\epsilon$
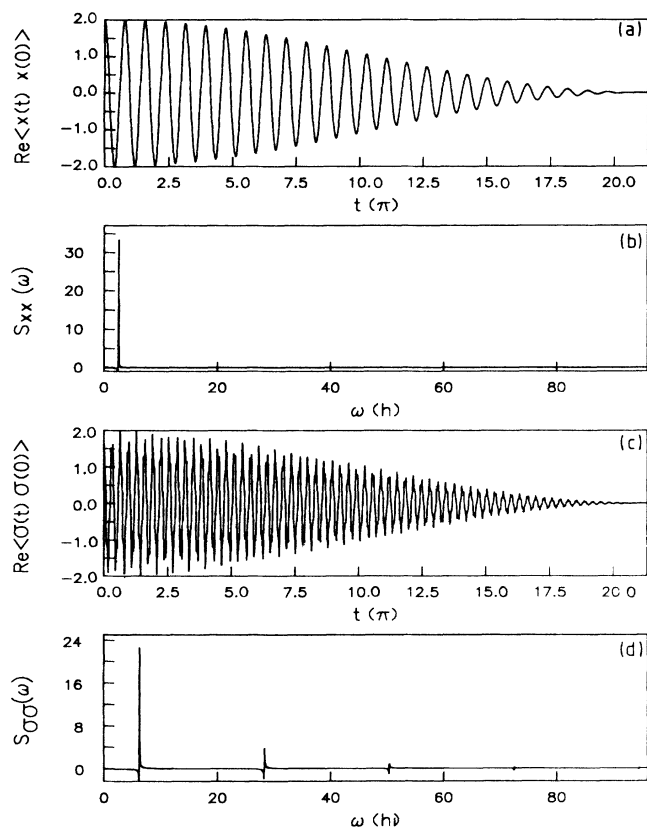


FIG. 3. Real part of the time-correlation functions $\langle x(t)x(0)\rangle$ (a) and $\langle\sigma^z(t)\sigma^z(0)\rangle$ (c) for the two-level system quadratically coupled to a harmonic oscillator as described by (3.4) ($\Omega=8$, $h=1$, $C_2=0.9$, and $N=30$). The time-correlation functions have been multiplied by a Hanning window as given by (3.9). The spectral functions $\mathscr{S}_{xx}(\omega)$ (b) and $\mathscr{S}_{\sigma\sigma}(\omega)$ (d), obtained through fast-Fourier transformation, are also shown. Note that the oscillator spectrum shows only one signal, whereas the tunneling spectrum consists of at least four visible peaks.
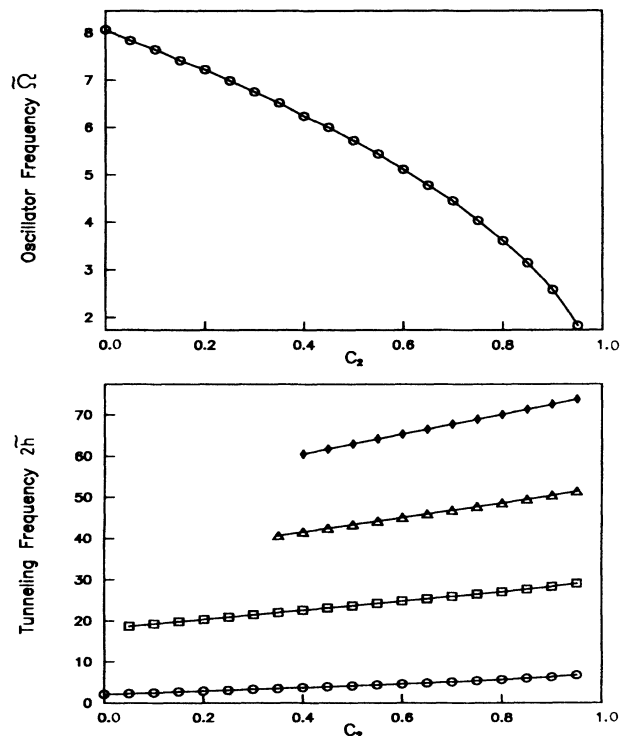


FIG. 4. Behavior of the peak positions $\tilde{\Omega}$ and $2\tilde{h}$ in the oscillator and tunneling spectra $\mathscr{S}_{xx}$ and $\mathscr{S}_{\sigma\sigma}$ as a function of the coupling constant $C_2$ for the model (3.4). Except for $C_2$, all parameters are the same as for Fig. 3. The curves are seen to fit with the theoretically expected results $\tilde{\Omega}=\Omega(1-C_2)^{1/2}$ and $2\tilde{h}(m)=2h+(2m+1/2)\Omega(1+C_2)^{1/2}-\tfrac{1}{2}\Omega(1-C_2)^{1/2}$ with $m=0$ (circles), $m=1$ (squares), $m=2$ (triangles), and $m=3$ (diamonds).

and $T \otimes \tau_2$, respectively).[25] These systems have been discussed extensively in the reviews and texts of Sturge,[26] Ham,[27] Abragam and Bleaney,[28] Englman,[29] and more recently Bates.[12] All except for the last reference treat the JT ion and its immediate neighbors as an almost isolated cluster, vibrating with an effective frequency. Within the same cluster approximation we will employ the approach presented in Sec. II as a unified method, valid in all coupling regimes, to solve the vibronic problem of these JT systems. Indeed, the presence of orbital degeneracy, which invalidates the assumption that the vibrational and electronic problems can be solved separately, requires the entire "vibronic" problem to be solved as a whole, evidently within the few-level approximation for the orbital multiplet.[29] As such, the electronic degeneracy is replaced by a vibronic degeneracy of the same symmetry type but for which the electronic properties differ quantitatively from those of the uncoupled system. These differences are expressed through the matrix elements of electronic operators between the vibronic states and are commonly referred to as the Ham reduction factors.[30,31] Another quantity of physical importance is the energy spectrum of the coupled system, especially the low-energy differences, as they govern the transition from dynamic to static JT effects in the limit of strong coupling.[27] In what follows, we will evaluate the energy differences as well as some Ham factors for the cubic JT systems $T \otimes \epsilon$, $T \otimes \tau_2$, and $E \otimes \epsilon$. Although most of the results presented here are already known through other methods, we choose to treat these systems, as they illustrate in a nontrivial way the method's applicability. A short synopsis of, and comparison with, the literature will be given. For the system $E \otimes \epsilon$, in addition to the EPM, an extra symmetry projector has to be introduced, as will be discussed in detail in Sec. IV C and in the Appendix.

## A. Orbital triplet ($T_1$ or $T_2$)—$E$ vibrational mode: $T \otimes \epsilon$

For an orbital triplet (e.g., $T_2$) in cubic symmetry, the linear JT coupling to an $E$ vibrational mode is given by the following Hamiltonian ($\hbar = 1$):[25]

$$\mathcal{H} = \mathcal{H}_{OO} + \mathcal{H}_{LO} , \qquad (4.1a)$$

with

$$\mathcal{H}_{OO} = a_\theta^\dagger a_\theta + a_\epsilon^\dagger a_\epsilon , \qquad (4.1b)$$

$$\mathcal{H}_{LO} = (C_1)^{1/2}[(a_\theta^\dagger + a_\theta)\mathscr{E}_\theta + (a_\epsilon^\dagger + a_\epsilon)\mathscr{E}_\epsilon] , \qquad (4.1c)$$

and

$$\mathscr{E}_\theta = \begin{bmatrix} -1/\sqrt{6} & 0 & 0 \\ 0 & -1/\sqrt{6} & 0 \\ 0 & 0 & 2/\sqrt{6} \end{bmatrix} ,$$

$$\mathscr{E}_\epsilon = \begin{bmatrix} 1/\sqrt{2} & 0 & 0 \\ 0 & -1/\sqrt{2} & 0 \\ 0 & 0 & 0 \end{bmatrix} , \qquad (4.1d)$$

which is clearly of the general form proposed in Sec. II. We have taken the oscillators' mass $M = 1$ and set the

frequency $\Omega = 1$. The conventional indexation $(\theta, \epsilon)$ is used for the components of the doublet, transforming as $(3z^2 - r^2)$ and $\sqrt{3}(x^2 - y^2)$, respectively. The matrices are given in the electronic representation $|\xi\rangle$, $|\eta\rangle$, $|\zeta\rangle$, transforming under the cubic symmetry operations as $yz$, $zx$, and $xy$ (for $T_2$). Some notational differences with the literature due to the use of Euclidean-normalized matrices and to the second-quantization formalism are resolved by the following substitutions: $V = l_\epsilon = -2(C_1/3)^{1/2}$.[25,30] Since $\mathcal{H}_{LO}$ does not mix the electronic states, the vibronic problem simplifies tremendously and can be solved analytically,[30] the eigenfunctions being given as a Born-Oppenheimer product of one of the electronic eigenfunctions $|\xi\rangle$, $|\eta\rangle$, $|\zeta\rangle$ with two displaced harmonic oscillator vibrational wave functions. The spectrum is that of a two-dimensional harmonic oscillator shifted by the JT-stabilization energy and therefore shows a partly spurious degeneracy. The ground-state vibronic triplet, denoted by $|\Psi_{T_\xi}\rangle$, $|\Psi_{T_\eta}\rangle$, $|\Psi_{T_\zeta}\rangle$ is, however, only triply degenerate and the following reduction factors have been calculated from the vibrational overlap integrals:[30]

$$K(E) = \langle \Psi_{T_\zeta} | \sqrt{3/2}\mathscr{E}_\theta | \Psi_{T_\zeta}\rangle = 1 , \qquad (4.2a)$$

$$K(T_1) = i\langle \Psi_{T_\xi} | \sqrt{2}\mathcal{L}_z | \Psi_{T_\eta}\rangle = \exp(-C_1) , \qquad (4.2b)$$

$$K(T_2) = \langle \Psi_{T_\xi} | \sqrt{2}\mathcal{T}_\zeta | \Psi_{T_\eta}\rangle = \exp(-C_1) , \qquad (4.2c)$$

with

$$\mathcal{L}_z = \begin{bmatrix} 0 & -i/\sqrt{2} & 0 \\ i/\sqrt{2} & 0 & 0 \\ 0 & 0 & 0 \end{bmatrix} ,$$

$$\mathcal{T}_\zeta = \begin{bmatrix} 0 & 1/\sqrt{2} & 0 \\ 1/\sqrt{2} & 0 & 0 \\ 0 & 0 & 0 \end{bmatrix} , \qquad (4.2d)$$

where the electronic operators $\mathcal{L}_z, \mathcal{T}_\zeta$ can be shown to belong to $T_1$ and $T_2$, respectively.

We treated (4.1) as described in Sec. II, performing the EPM with three vibronic states, and found numerical expressions for $|\Psi_{T_\xi}\rangle$, $|\Psi_{T_\eta}\rangle$, and $|\Psi_{T_\zeta}\rangle$. The resulting Ham factors (4.2) are presented in Table II for two different values for the number of states $N_\theta = N_\epsilon = N$ included in the oscillator representation. This finite dimension, together with the value of $b$ in the approximation on $e^{-\beta\mathcal{H}}$ determine the quality of the numerical approximation. All our data are presented for $b$ sufficiently small such that the numbers can be considered as having converged as a function of $b$. Typically $b = 0.01$ was used. From comparison with the exact values also listed in Table II, one notices that higher values of $N$ are required for increasing coupling strength $C_1$, as can be understood from the fact that $C_1$ determines the degree up to which the oscillators are displaced.

## B. Orbital triplet ($T_1$ or $T_2$)—$T_2$ vibrational mode: $T \otimes \tau_2$

If an orbital triplet (e.g., $T_2$) in cubic symmetry is coupled to a set of three vibrational modes belonging to $T_2$

TABLE II. The Ham reduction factors $K(T_1)=K(T_2)$ within the vibronic triplet ground state for the system of an orbital triplet $T_2$, linearly coupled to an $E$ vibrational mode $(T\otimes\epsilon)$. $N$ denotes the number of states used to approximate the $\theta$ and $\epsilon$ oscillator. From comparison with the analytic result $\exp(-C_1)$, it can be seen that higher values of $N$ are required for increasing linear coupling strength $C_1$.

| $C_1$ | $\exp(-C_1)$ | $K(T_1)$ | | $K(T_2)$ | |
|---|---|---|---|---|---|
| | | $N=5$ | $N=10$ | $N=5$ | $N=10$ |
| 0.5 | 0.6065 | 0.6067 | 0.6065 | 0.6066 | 0.6065 |
| 1.0 | 0.3679 | 0.3705 | 0.3679 | 0.3693 | 0.3679 |
| 1.5 | 0.2231 | 0.2308 | 0.2231 | 0.2267 | 0.2231 |
| 2.0 | 0.1353 | 0.1483 | 0.1353 | 0.1435 | 0.1353 |
| 2.4 | 0.0821 | 0.0986 | 0.0821 | 0.0930 | 0.0821 |
| 3.0 | 0.0498 | 0.0678 | 0.0498 | 0.0622 | 0.0498 |

and labeled with the indices $(\xi,\eta,\zeta)$, the vibronic Hamiltonian reads[25]

$$\mathcal{H}=\mathcal{H}_{OO}+\mathcal{H}_{LO}\ ,\qquad(4.3a)$$

with

$$\mathcal{H}_{OO}=a_\xi^\dagger a_\xi+a_\eta^\dagger a_\eta+a_\zeta^\dagger a_\zeta\ ,\qquad(4.3b)$$

$$\mathcal{H}_{LO}=(C_1)^{1/2}[(a_\xi^\dagger+a_\xi)\mathcal{T}_\xi+(a_\eta^\dagger+a_\eta)\mathcal{T}_\eta$$
$$+(a_\zeta^\dagger+a_\zeta)\mathcal{T}_\zeta]\ ,\qquad(4.3c)$$

and

$$\mathcal{T}_\xi=\begin{bmatrix}0&0&0\\0&0&1/\sqrt{2}\\0&1/\sqrt{2}&0\end{bmatrix}\ ,$$

$$\mathcal{T}_\eta=\begin{bmatrix}0&0&1/\sqrt{2}\\0&0&0\\1/\sqrt{2}&0&0\end{bmatrix}\ ,\qquad(4.3d)$$

$$\mathcal{T}_\zeta=\begin{bmatrix}0&1/\sqrt{2}&0\\1/\sqrt{2}&0&0\\0&0&0\end{bmatrix}\ ,$$

again in units of $M=\Omega=\hbar=1$. The matrices are relative to the previously introduced set $|\xi\rangle,|\eta\rangle,|\zeta\rangle$, and the relation with equivalent notations in the literature is given by $-V=l_\tau=k=(C_1)^{1/2}$.[25,30,32] As the electronic operators do not commute, a separation of vibrational and electronic coordinates is not possible and a general solution to the problem can only be found by numerical

determination of a linear combination of symmetry-adapted products of three-dimensional oscillator wave functions with a set of electronic functions.[29,32] For the two limiting cases of strong and weak coupling, analytic expressions for the eigenvalues have also been derived.[25]

As it is known[32] that in the strong-coupling regime an $A_1$ singlet $|\Psi_{A_1}\rangle$ approaches the $T_2$ ground triplet $|\Psi_{T_\xi}\rangle,|\Psi_{T_\eta}\rangle,|\Psi_{T_\zeta}\rangle$, we performed an EPM calculation on (4.3) using four states. Within the triplet we evaluated the reduction factors $K(E)$, $K(T_1)$, and $K(T_2)$ in the same way as for the case $T\otimes\epsilon$ previously described. The values listed in Table III are in agreement with the curves of Ref. 32. The knowledge of the singlet state $|\Psi_{A_1}\rangle$ allows the evaluation of yet another reduction factor:

$$R(T_2)=\langle\Psi_{A_1}|\sqrt{2}\mathcal{T}_\xi|\Psi_{T_\xi}\rangle\ ,\qquad(4.4)$$

since a $T_2$ electronic operator makes transitions between the $T_2$ electronic triplet $|\xi\rangle,|\eta\rangle,|\zeta\rangle$ and the electronic singlet $|A_1\rangle$ and consequently also from the vibronic states $|\Psi_{T_\xi}\rangle,|\Psi_{T_\eta}\rangle,|\Psi_{T_\zeta}\rangle$ to $|\Psi_{A_1}\rangle$. Note that $T_1$ and $E$ electronic operators show no such transitions, although for an orbital $T_1$ singlet, all indices 1 and 2 should be interchanged. We finally list in Table III the energy difference $\Delta$ between the first-excited singlet and ground-state triplet, also in agreement with Ref. 32. The approach of the singlet to the ground state at high coupling strengths is interpreted[30] as a transition from a dynamic to a static JT system, thereby associating the

TABLE III. The Ham reduction factors $K(E),K(T_1),K(T_2)$ within the vibronic triplet ground state for the system of an orbital triplet $T_2$, linearly coupled to a $T_2$ vibrational mode $(T\otimes\tau_2)$. As the coupling strength $C_1$ increases, the energy difference $\Delta$ between the ground triplet and first-excited singlet decreases, while the reduction factor $R(T_2)$ between these low-energy eigenstates increases. The values of $K(E)$, $K(T_1)$, $K(T_2)$, and $\Delta$ are in excellent agreement with the results of Ref. 32. The calculation was done for $N_\xi=N_\eta=N_\zeta=10$, which is sufficiently large for the range of $C_1$ covered.

| $C_1$ | $K(E)$ | $K(T_1)$ | $K(T_2)$ | $R(T_2)$ | $\Delta$ |
|---|---|---|---|---|---|
| 0.5 | 0.55 | 0.54 | 0.84 | 0.28 | 0.70 |
| 1.0 | 0.37 | 0.34 | 0.76 | 0.33 | 0.54 |
| 1.5 | 0.27 | 0.23 | 0.72 | 0.36 | 0.43 |
| 2.0 | 0.20 | 0.16 | 0.69 | 0.37 | 0.35 |
| 2.4 | 0.16 | 0.11 | 0.67 | 0.39 | 0.28 |
| 3.0 | 0.12 | 0.08 | 0.66 | 0.40 | 0.22 |

quadruplet thus formed with the four equivalent trigonal distortions found for the static problem.[33] The energy separation $\Delta$ can then be seen as representing a barrier height through which the low-energy states in each distorted configuration interact. As can be seen from Table III, $R(T_2)$ grows with increasing coupling strength.

### C. Orbital doublet $(E)$—$E$ vibrational mode: $E \otimes \epsilon$

The full vibronic Hamiltonian for a doublet electronic state $E$ with quadratic JT coupling to an $E$ vibrational mode in cubic symmetry is given by ($\hbar = 1$) (Refs. 25 and 34)

$$\mathcal{H} = \mathcal{H}_{OO} + \mathcal{H}_{LO} + \mathcal{H}_{LOO} , \qquad (4.5a)$$

with

$$\mathcal{H}_{OO} = a_\theta^\dagger a_\theta + a_\epsilon^\dagger a_\epsilon , \qquad (4.5b)$$

$$\mathcal{H}_{LO} = (C_1)^{1/2}[(a_\theta^\dagger + a_\theta)\mathcal{U}_\theta + (a_\epsilon^\dagger + a_\epsilon)\mathcal{U}_\epsilon] , \qquad (4.5c)$$

$$\mathcal{H}_{LOO} = \frac{C_2}{4\sqrt{2}}\{[(a_\theta^\dagger + a_\theta)^2 - (a_\epsilon^\dagger + a_\epsilon)^2]\mathcal{U}_\theta$$
$$- 2(a_\theta^\dagger + a_\theta)(a_\epsilon^\dagger + a_\epsilon)\mathcal{U}_\epsilon\} , \qquad (4.5d)$$

and

$$\mathcal{U}_\theta = \begin{bmatrix} 1/\sqrt{2} & 0 \\ 0 & -1/\sqrt{2} \end{bmatrix} ,$$

$$\mathcal{U}_\epsilon = \begin{bmatrix} 0 & -1/\sqrt{2} \\ -1/\sqrt{2} & 0 \end{bmatrix} , \qquad (4.5e)$$

with again for the oscillators $M = \Omega = 1$. The $(2 \times 2)$ matrices are given in the electronic representation $|\theta\rangle, |\epsilon\rangle$, transforming as $(3z^2 - r^2)$ and $\sqrt{3}(x^2 - y^2)$ under the cubic group. The system $E \otimes \epsilon$ is by far the one on which most of the experimental work has been done and for which the theory is most complete. We found it instructive to give a synopsis of the theoretical results obtained over the past 15 years by various methods. The presentation here is of an enumerating nature and the previously mentioned review literature and references therein should be consulted for more details. For the ease of comparison, $(C_1)^{1/2}$ is related to $-L/2$ of Ref. 29 in which one can find further connections to other references.

General solutions of the linear problem $\mathcal{H}_{OO} + \mathcal{H}_{LO}$ have been found with vibronic functions whose electronic parts, conveniently denoted as $|+\rangle, |-\rangle$, are the eigensolutions of the static problem and therefore diagonalize the electronic part of $\mathcal{H}_{LO}$. The vibrational functions are determined by coupled differential equations which, by numerical solution, allow the determination of the energy spectrum[35] and Ham factors[34] defined as follows:[31]

$$\Delta_1 = E(\Psi_A) - E(\Psi_E) , \qquad (4.6a)$$

$$q_{11} = \langle \Psi_{E_\theta} | \sqrt{2}\mathcal{U}_\theta | \Psi_{E_\theta}\rangle , \qquad (4.6b)$$

$$p_{11} = i\langle \Psi_{E_\theta} | \sqrt{2}\mathcal{A}_2 | \Psi_{E_\epsilon}\rangle , \qquad (4.6c)$$

with

$$\mathcal{A}_2 = \begin{bmatrix} 0 & -i/\sqrt{2} \\ i/\sqrt{2} & 0 \end{bmatrix} , \qquad (4.6d)$$

where the electronic operator $\mathcal{A}_2$ (relative to $|\theta\rangle, |\epsilon\rangle$) belongs to the $A_2$ representation of the cubic group. The vibronic ground doublet $|\Psi_{E_\theta}\rangle, |\Psi_{E_\epsilon}\rangle$ is indexed in the usual way and the first-excited state is temporarily denoted as $|\Psi_A\rangle$. In addition to the general numerical treatment, analytic results for $p$ and $q$ are known for the small-coupling[31] and strong-coupling regimes.[36] In the latter limit, $\mathcal{H}_{LO}$ (diagonal relative to $|+\rangle, |-\rangle$) starts to dominate the off-diagonal kinetic energy part in $\mathcal{H}_{OO}$ (angular momentum), and the system is said to make a transition from the dynamic to the static regime. The general vibronic wave functions can be seen to become dominated by either the part with $|+\rangle$ or $|-\rangle$, depending on the sign of $\mathcal{H}_{LO}$, but clearly become well represented by an adiabatic Born-Oppenheimer form.

A serious drawback of the linear model, as it stands, is the accidental degeneracy ($|\Psi_A\rangle$ as an $A$-transforming vibronic function is in fact doubly degenerate) which can only be lifted through the inclusion of higher-order "warping" terms in the Hamiltonian. O'Brien[37] treated an electronically diagonal third-order oscillator anharmonicity $\mathcal{H}_{OOO}$ only within the adiabatic limit of strong linear coupling. Williams et al.[36] performed a first-order perturbation calculation on the influence of the nonadiabatic quadratic JT interaction $\mathcal{H}_{LOO}$ (4.5d) (notational relation: $4V_2 = C_2$) as well as of the nonadiabatic corrections from the kinetic energy, neglected by O'Brien. It is common to present these warping effects as a function of the barrier-height $\beta/\alpha$ that they introduce in the otherwise (accidentally) axial-symmetric angular dependence of the static potential. Within the notations of our work

$$\beta/\alpha = C_1^2 C_2/2 . \qquad (4.7)$$

More recently, the warping effects, both of the type $\mathcal{H}_{LOO}$ and $\mathcal{H}_{OOO}$, have been treated through numerical diagonalization procedures by Hoffman and Estle[38] and Sakamoto[39,40] for a wide range of linear coupling strengths. It is interesting to discuss these treatments in some detail as, although they are far from equivalent to the technique proposed in this work, some common characteristics can be found. Following Sec. II, we treat the Hamiltonian (4.5) in the representation $|n_\theta n_\epsilon S\rangle$, where $n_\theta$ and $n_\epsilon$ are the harmonic excitation numbers for the $\theta$ and $\epsilon$ partners of the vibrational mode and $|S\rangle = |\theta\rangle, |\epsilon\rangle$ denotes the electronic state. As already pointed out,[38] within this representation the Hamiltonian matrix is fairly dense and does not therefore enable a "brute force" diagonalization approach. The powerfulness of the product-formula approach is due precisely to the fact that it circumvents the problem of diagonalizing matrices. In Ref. 38 the authors opted for another representation in which the Hamiltonian matrix is more sparse. They generated the so-called zero-coupling basis states[35] in which the linear system $\mathcal{H}_{OO} + \mathcal{H}_{LO}$ is represented by a semi-infinite number of blocks of semi-infinite tridiagonal matrices. For a given value of the linear coupling constant the representation was truncated

and each tridiagonal matrix was then diagonalized numerically. Within the set of linear-coupling eigenfunctions the warping interactions introduced off-diagonal matrix elements which were determined through induction.[38] The resulting matrix could then be diagonalized numerically. As the linear-coupling basis states could be classified according to the irreducible representations $\Gamma^{E_\theta}$, $\Gamma^{E_\epsilon}$, $\Gamma^{A_2}$, and $\Gamma^{A_1}$ of the cubic group, the final matrix could be split into four blocks.

It turned out in our calculations that this symmetry classification was very valuable in the cases where a singlet ($A_1$ or $A_2$) became nearly degenerate with a doublet $E$; for in this situation the EPM did yield three orthogonal states with correct energies but with a symmetry which became very difficult to pin down. We have investigated this aspect by evaluating the expectation values of the following vibronic operator:

$$\Theta = (a_\theta^\dagger + a_\theta)\mathcal{U}_\theta - (a_\epsilon^\dagger + a_\epsilon)\mathcal{U}_\epsilon , \qquad (4.8)$$

which can be seen to transform as the $\theta$ component of an $E$ representation under the simultaneous transformation of vibrational and electronic coordinates. Note the formal analogy between $\Theta$ and the vibrational part accompanying $\mathcal{U}_\theta$ in (4.5d). Group theoretically, the matrix elements of $\Theta$ between the four possible vibronic states $|\Psi_{E_\theta}\rangle$, $|\Psi_{E_\epsilon}\rangle$, $|\Psi_{A_1}\rangle$, and $|\Psi_{A_2}\rangle$ are seen to be zero or nonzero (denoted by $*$) as follows:

$$
\begin{array}{c c c c c}
 & |\Psi_{E_\theta}\rangle & |\Psi_{E_\epsilon}\rangle & |\Psi_{A_1}\rangle & |\Psi_{A_2}\rangle \\
\langle\Psi_{E_\theta}| & * & 0 & * & 0 \\
\langle\Psi_{E_\epsilon}| & 0 & * & 0 & * \\
\langle\Psi_{A_1}| & * & 0 & 0 & 0 \\
\langle\Psi_{A_2}| & 0 & * & 0 & 0
\end{array} \qquad (4.9)
$$

The loss of symmetry then manifests itself as nonzero matrix elements. To cope with this problem we have applied an additional symmetry projector in combination with the EPM. We refer to the Appendix for a detailed description of this projector. Let it suffice here to state that its action on an eigenfunction filters out all parts which do not belong to a specified irreducible representation. Therefore, in combination with the EPM working on $d$ initially random states, we find the $d$ lowest-energy eigenstates of a predetermined symmetry. In general, these states are different from the $d$ lowest-energy eigenstates found with the EPM.

As an illustration, we reproduced some of the results of Ref. 38. The notations used in Ref. 38 are $K_L = (C_1/2)^{1/2}$ and $K_N = C_2/8$. Notice that the $A_1$ and $A_2$ symmetry classification is interchanged due to a different sign in both the electronic operators $\mathcal{U}_\theta$ and $\mathcal{U}_\epsilon$. In Table IV we present the low-energy eigenvalues for a system with $C_1 = 18$ ($K_L = 3$) and $C_2 = \frac{10}{162}$ and $\frac{30}{162}$ corresponding to $\beta/\alpha = 10$ and 30. The runs were made with $b = 0.001$ and $N_\theta = N_\epsilon = 30$. It can be seen that the eigenvalue differences are in perfect agreement with the values presented in Fig. 3(a) of Ref. 38. It is our general experi-

ence with the EPM that a correct eigenvalue can, however, be found with a relatively inaccurate eigenstate; see, e.g., the problem of symmetry mixing previously mentioned. We therefore checked the eigenfunctions through evaluation of some Ham-reduction factors generally defined as follows:[38]

$$p_{kl} = \langle k, \Psi_{E_\theta} | i\sqrt{2}\mathcal{A}_2 | l, \Psi_{E_\theta}\rangle , \qquad (4.10\text{a})$$

$$q_{kl} = \langle k, \Psi_{E_\theta} | \sqrt{2}\mathcal{U}_\theta | l, \Psi_{E_\theta}\rangle , \qquad (4.10\text{b})$$

$$r_{kl} = -\langle k, \Psi_{E_\theta} | \sqrt{2}\mathcal{U}_\theta | l, \Psi_{A_1}\rangle , \qquad (4.10\text{c})$$

$$r'_{kl} = \langle k, \Psi_{E_\theta} | \sqrt{2}\mathcal{U}_\epsilon | l, \Psi_{A_2}\rangle , \qquad (4.10\text{d})$$

$$s_{kl} = -\langle k, \Psi_{A_1} | i\sqrt{2}\mathcal{A}_2 | l, \Psi_{A_2}\rangle . \qquad (4.10\text{e})$$

The extra subscripts $k, l$ label the states, the ground state corresponding to $k = 1$. As shown in Table IV, we assume the indexation to be made again for each value of $C_1$ and $C_2$. As a consequence, when a level crossing takes place, the indexation of some Ham factors abruptly changes. A possible way to overcome this inconvenience would be to label the states within each of the symmetry classes separately. However, to allow for a direct comparison with previous work, we will adopt the conventions of Ref. 38.

Table V lists some calculated Ham factors. They are to be compared with Fig. 5 of Ref. 38. Apart from some internal consistencies, which were respected, the signs of the reduction factors cannot be compared since $|\Psi\rangle$ and $-|\Psi\rangle$ are indistinguishable eigenstates. We therefore present absolute values in Table V. It should be pointed out that the labeling of our $r$- and $r'$-reduction factors is the same as in Ref. 38; this in spite of the interchange of the $A_1$ and $A_2$ labels. We believe this to be due to a notational inconsistency in Ref. 38, as one can easily see from the symmetry labeling in their Fig. 3(a). The discrepancy between the $r'_{42}$ and $r'_{12}$ values of Table V and the curves labeled as $|r'_{24}|$ and $-|r'_{12}|$ in Fig. 5 of Ref. 38 can also be traced back to Ref. 38, assuming an incorrect notation. Our $r'_{42}$ results are much closer to

TABLE IV. Low-energy eigenvalues ($E$) together with the symmetry ($\Gamma$) of the corresponding eigenstates for the Jahn-Teller system $E \otimes \epsilon$ [cf. Eq. (4.5)] with a linear coupling constant $C_1 = 18$ and for two values of the quadratic warping strength $C_2 = \frac{10}{162}$, $\frac{30}{162}$. The data are obtained from different EPM runs, one for each of the symmetries $A_1$, $A_2$, $E_\theta$, and $E_\epsilon$. All calculations are performed with $b = 0.001$ and $N = 30$.

| Index | $C_2 = \frac{10}{162}$ | | $C_2 = \frac{30}{162}$ | |
| --- | --- | --- | --- | --- |
| | $E(\Omega = 1)$ | $\Gamma$ | $E(\Omega = 1)$ | $\Gamma$ |
| 1 | $-9.62$ | $E$ | $-10.1$ | $E$ |
| 2 | $-9.61$ | $A_2$ | $-10.1$ | $A_2$ |
| 3 | $-9.35$ | $A_1$ | $-9.55$ | $A_1$ |
| 4 | $-9.30$ | $E$ | $-9.54$ | $E$ |
| 5 | $-9.12$ | $E$ | $-9.24$ | $E$ |
| 6 | $-8.92$ | $A_2$ | $-9.23$ | $A_2$ |
| 7 | $-8.91$ | $A_1$ | $-8.96$ | $E$ |
| 8 | $-8.58$ | $E$ | $-8.93$ | $A_2$ |

TABLE V. Absolute values of some Ham-reduction factors as defined in Eq. (4.10) for the Jahn-Teller system $E \otimes \epsilon$, using the same parameters as in Table IV. $s$- and $p$-type reduction factors are negligibly small and therefore not shown.

|  | $\|q_{11}\|$ | $\|q_{44}\|$ | $\|q_{14}\|$ | $\|r'_{12}\|$ | $\|r'_{42}\|$ | $\|r_{13}\|$ | $\|r_{43}\|$ |
|---|---|---|---|---|---|---|---|
| $C_2 = \frac{10}{162}$ | 0.49 | 0.29 | 0.11 | 0.67 | 0.22 | 0.22 | 0.65 |
| $C_2 = \frac{30}{162}$ | 0.49 | 0.47 | 0.087 | 0.70 | 0.12 | 0.12 | 0.67 |

their $-\|r'_{12}\|$ curve as well as are the $r'_{12}$ data to the $\|r'_{24}\|$ curve, although even then some discrepancies seem to persist. The value $r'_{12} = 0.70$ at $C_2 = \frac{30}{162}$ lies considerably above the upper limit $\|r'_{24}\|$ of Ref. 38. In fact, we verified through an intermediate calculation near $\beta/\alpha = 20$ that our values of $\|r'_{12}\|$ monotonously increase with $C_2$; this is contrast to the $\|r'_{24}\|$ curve of Ref. 38. We would finally like to comment on the relatively large discrepancy of the $r'_{42}$ and $r_{13}$ data with the $-\|r'_{12}\|$ and $-\|r_{13}\|$ curves, respectively, while the other Ham factors, such as the $q$'s and $r_{43}$, are in much better agreement. It is in fact observed that our data are much closer to the corresponding dashed lines of Fig. 5,[38] which represent the authors' data for the case of anharmonic warping, in contrast to the quadratic warping (solid lines). The authors claim both types of warping to be indistinguishable for all investigated Ham factors, except for the $-\|r'_{12}\|$ and $-\|r_{13}\|$ curves; henceforth the distinction in their paper with a solid and a dashed line. As we did not consider an $\mathcal{H}_{OOO}$ term in the Hamiltonian we cannot investigate this question any further.

It should finally be mentioned that we also reproduced some of the results of Ref. 40. The notational relation is $V_1 = (C_1)^{1/2}$ and $V_2 = C_2/4$, where the indexation of $A_1$ and $A_2$ is again expected to be interchanged due to a change of sign in the operators $\mathcal{U}_\theta$ and $\mathcal{U}_\epsilon$. No results are presented here for this comparison, as we found good agreement, both in the eigenvalues as well as in the examined reduction factors ($r_{43}$, $q_{14}$, and $q_{44}$).

## V. CONCLUSION

A symmetrized Trotter-Suzuki approximation on $e^{-\beta H}$ (or on $e^{-it\mathcal{H}}$) has been proposed for $\mathcal{H}$ representing a few-level system coupled both linearly and quadratically to a finite collection of harmonic oscillators. We have illustrated the extended projector method by applying it to a pseudo-Jahn-Teller system consisting of a two-level system quadratically coupled to a single harmonic oscillator. This system is shown to be unstable as a function of the coupling strength, and its ground-state dynamic properties are shown to differ substantially from those of an analogous system with linear coupling. Furthermore, we examined the low-energy eigenstates of the cubic Jahn-Teller systems $T \otimes \epsilon$ and $T \otimes \tau_2$ and also of the system $E \otimes \epsilon$ for which we included a quadratic warping interaction. Apart from some details, the results are in agreement with the existing literature on these systems. In connection with the study of $E \otimes \epsilon$, a symmetry projector has been introduced.

## APPENDIX

As the projector to be worked out here is based on some general group-theoretical theorems, we will start with a short synopsis of some formulas, the proof of which can be found in any handbook on group theory (e.g., Ref. 15). The projection operator $\mathcal{P}_\lambda^{(j)}$ which selects out of any function $F$ the part belonging to the $\lambda$th row of the $j$th representation is known to be given by

$$\mathcal{P}_\lambda^{(j)} F = (l_j/h) \sum_R \Gamma_{\lambda\lambda}^{(j)}(R)^* P_R F , \qquad (A1)$$

in which $\Gamma^{(j)}(R)$ is the $l_j$-dimensional irreducible matrix of the $j$th represenation, corresponding to the symmetry operation $R$. The summation over $R$ covers all $h$ symmetry elements in the group under study. $P_R$ denotes the action of the symmetry operation $R$ on the function $F$. A function $\phi_\kappa^{(i)}$ is said to be a basis function belonging to the $\kappa$th row of the $i$th representation (dimension $l_i$) if it transforms among its partners under the symmetry operation $R$ as prescribed by

$$P_R \phi_\kappa^{(i)} = \sum_{\mu=1}^{l_i} \phi_\mu^{(i)} \Gamma_{\mu\kappa}^{(i)}(R) . \qquad (A2)$$

For the situation encountered with the $E \otimes \epsilon$ JT system, the symmetry group is $O$ with $h = 24$. The occurring irreducible matrices $\Gamma^E$ ($l = 2$) and $\Gamma^{A_1}, \Gamma^{A_2}$ ($l = 1$) are known to be real and can be found in textbooks. The corresponding symmetry projectors are $\mathcal{P}_\theta^E$, $\mathcal{P}_\epsilon^E$, $\mathcal{P}^{A_1}$, and $\mathcal{P}^{A_2}$, where we suppressed the index $\lambda = 1$ for the one-dimensional representations and adopted the conventional $\theta, \epsilon$ to label the $E$ representation.

A general wave function, as it is obtained from the EPM calculation, is conveniently written in the basis $\|n_\theta n_\epsilon S\rangle$ with $n_\theta, n_\epsilon$ the excitation numbers of the $\theta$ and $\epsilon$ partners of the vibrational motion and $\|S\rangle = \|\theta\rangle, \|\epsilon\rangle$ denoting the electronic states. Under the assumption

that the irreducible matrices are known, it can be seen from Eq. (A1) that the action of any symmetry projector $\mathcal{P}$ is fully determined by the knowledge of

$$P_R \mid n_\theta n_\epsilon S \rangle = P_R \mid n_\theta n_\epsilon \rangle P_R \mid S \rangle , \qquad (A3)$$

where we used the direct-product property of $P_R$. The electronic part $P_R \mid S \rangle$ is simple as by construction the two possible values of $\mid S \rangle$ are known to transform as either the $\theta$ or $\epsilon$ partners of an $E$ representation. Therefore, following (A2) one can write

$$P_R \mid \theta \rangle = \Gamma_{\theta\theta}^E(R) \mid \theta \rangle + \Gamma_{\epsilon\theta}^E(R) \mid \epsilon \rangle ,$$
$$P_R \mid \epsilon \rangle = \Gamma_{\theta\epsilon}^E(R) \mid \theta \rangle + \Gamma_{\epsilon\epsilon}^E(R) \mid \epsilon \rangle . \qquad (A4)$$

For the vibrational part the situation is somewhat more complex. Knowing the transformation properties of

$q_\theta \sim (a_\theta^\dagger + a_\theta)$, $q_\epsilon \sim (a_\epsilon^\dagger + a_\epsilon)$ and thus also of the conjugate momenta $p_\theta$ and $p_\epsilon$, one has again by construction

$$P_R a_\theta^\dagger = \Gamma_{\theta\theta}^E(R) a_\theta^\dagger + \Gamma_{\epsilon\theta}^E(R) a_\epsilon^\dagger ,$$
$$P_R a_\epsilon^\dagger = \Gamma_{\theta\epsilon}^E(R) a_\theta^\dagger + \Gamma_{\epsilon\epsilon}^E(R) a_\epsilon^\dagger , \qquad (A5)$$

with an analogous formula for the annihilation operators $a_\theta$ and $a_\epsilon$. The difficulty lies in the fact that Eq. (A5) only prescribes the transformation properties of linear forms in the creation operators, whereas according to $\mid n \rangle = (n!)^{-1/2} (a^\dagger)^n \mid 0 \rangle$, one needs to know $P_R (a^\dagger)^n$ for $n$ any excitation number. As a limit of the direct-product property it can be seen, however, that $P_R (a^\dagger)^n = (P_R a^\dagger)^n$, which reduces the problem to a power of the known transformation properties of $a^\dagger$. Applying the binomial formula one then finds

$$P_R \mid n_\theta n_\epsilon \rangle = c_1 \left[ \sum_{m_\theta=0}^{n_\theta} (\Gamma_{\theta\theta}^E a_\theta^\dagger)^{m_\theta} (\Gamma_{\epsilon\theta}^E a_\epsilon^\dagger)^{n_\theta - m_\theta} \right] \left[ \sum_{m_\epsilon=0}^{n_\epsilon} (\Gamma_{\theta\epsilon}^E a_\theta^\dagger)^{m_\epsilon} (\Gamma_{\epsilon\epsilon}^E a_\epsilon^\dagger)^{n_\epsilon - m_\epsilon} \right] \mid 00 \rangle , \qquad (A6a)$$

$$P_R \mid n_\theta n_\epsilon \rangle = c_1 \sum_{m_\theta, m_\epsilon=0}^{n_\theta, n_\epsilon} c_2 (\Gamma_{\theta\theta}^E)^{m_\theta} (\Gamma_{\theta\epsilon}^E)^{m_\epsilon} (\Gamma_{\epsilon\theta}^E)^{n_\theta - m_\theta} (\Gamma_{\epsilon\epsilon}^E)^{n_\epsilon - m_\epsilon} \mid m_\theta + m_\epsilon \, n_\theta + n_\epsilon - m_\theta - m_\epsilon \rangle , \qquad (A6b)$$

where we have suppressed the $R$ dependences in the right-hand side and where

$$c_1 = 1/\sqrt{n_\theta! n_\epsilon!} ,$$
$$c_2 = \sqrt{(m_\theta + m_\epsilon)!(n_\theta + n_\epsilon - m_\theta - m_\epsilon)!} .$$

Expression (A6b) can be programmed rather efficiently in an inductive way. From (A1) and (A6b) it is seen that the projection of a complete wave function, involving the action of all 24 $P_R$ on all possible $\mid n_\theta n_\epsilon \rangle$ scales as 24 $[N(N+1)/2]^2$, assuming we confine ourselves to a finite-dimensional representation $\mid 0 \rangle, \ldots, \mid N \rangle$ for both the $\theta$ and $\epsilon$ oscillator. Related to this number of operations, one further optimization should be mentioned. As can be seen from (A6b), the action of $P_R$ consists in a redistribution of $\mid n_\theta n_\epsilon \rangle$ among all possible $\mid n_\theta' n_\epsilon' \rangle$ for which $n_\theta' + n_\epsilon' = n_\theta + n_\epsilon$, i.e., $\theta$- and $\epsilon$ excitations are interchanged, provided the total degree of excitation is conserved. In practice, however, due to the finite-dimensional representation, the full summation of (A6b) cannot be carried out for those $\mid n_\theta n_\epsilon \rangle$ for which $n_\theta + n_\epsilon > N$ because one simply does not have all required excited states within the representation. This results in a partial loss of the norm of the wave function. We have examined this effect in detail and have seen that if $N$ is chosen sufficiently large, which is of course the appropriate solution to this inherent numerical problem, one finds that already after very few symmetry projections the weight of the parts $\mid n_\theta n_\epsilon \rangle, n_\theta + n_\epsilon > N$ becomes negligible compared to the rest of the wave function. An evi-

dent optimization of the projector therefore consists in setting $P_R \mid n_\theta n_\epsilon \rangle = 0$ if $n_\theta + n_\epsilon > N$ instead of evaluating the laborious summations in (A6b). In this way roughly half of the elements of the wave function have to be handled, yielding considerable reduction in CPU time. In a typical case ($N = 30$) the action of a complete symmetry projection $\mathcal{P}$ for the JT system $E \otimes \epsilon$ took 1.5 min of CPU time on a VAX 8200 computer. As one can carry out many EPM steps for one symmetry projection, this is not a bottle neck as far as total CPU time is concerned, and we therefore did not seek further optimizations.

A far larger amount of calculations could be saved by noticing that only through a very minor modification the projection $\mathcal{P}_\lambda^{(j)}$ could be transformed into a generator $\mathcal{P}_{\lambda\kappa}^{(j)}$ which, by operating on $\phi_\kappa^{(j)}$ can be shown[15] to result in $\phi_\lambda^{(j)}$

$$\mathcal{P}_{\lambda\kappa}^{(j)} \phi_\kappa^{(j)} = (l_j/h) \sum_R \Gamma_{\lambda\kappa}^{(j)}(R)^* P_R \phi_\kappa^{(j)} = \phi_\lambda^{(j)} . \qquad (A7)$$

Applied to a doublet $E$ in the system $E \otimes \epsilon$, a considerable improvement in efficiency resulted through use of this trick, as only one partner had to be determined with an EPM run. The other one could then be generated out of it. As a final remark we would like to mention that the technique developed here in connection with excited states of a two-dimensional $E$ representation is more general and can easily be extended to any situation in which one needs to know the transformation properties of nonlinear functions of representational basis functions.

[1]R. Pirc and J. A. Krumhansl, Phys. Rev. B 11, 4470 (1975).

[2]T. Holstein, Ann. Phys. (N.Y.) 8, 343 (1959).

[3]S. Shore and L. M. Sander, Phys. Rev. B 7, 4537 (1973).

[4]N. Rivier and T. J. Coe, J. Phys. C 10, 4471 (1977).

[5]P. Prelovšek, J. Phys. C 12, 1855 (1979).

[6]R. Beck, W. Götze, and P. Prelovšek, Phys. Rev. A 20, 1140 (1979).

[7]S. Shore and L. M. Sander, Phys. Rev. B 12, 1546 (1975).

[8]B. G. Dick, Phys. Rev. B 16, 3359 (1977).

[9]M. Wagner and J. Vázquez-Márquez, Solid State Commun. 60, 781 (1986).

[10]V. Denner and M. Wagner, J. Phys. C 17, 153 (1984).

[11]S. Benk and E. Sigmund, J. Phys. C 18, 533 (1985).

[12]C. A. Bates, Phys. Rev. C 35, 187 (1978).

[13]R. Loudon, The Quantum Theory of Light (Clarendon, Oxford, England, 1973).

[14]M. Vanhimbeeck, H. De Raedt, and D. Schoemaker, Phys. Rev. A 36, 4612 (1987).

[15]M. Tinkham, Group Theory and Quantum Mechanics (McGraw-Hill, New York, 1964).

[16]H. De Raedt and B. De Raedt, Phys. Rev. A 28, 3575 (1983).

[17]M. Suzuki, J. Math. Phys. 26, 601 (1985).

[18]M. Suzuki, Commun. Math. Phys. 51, 183 (1976).

[19]M. Suzuki, Phys. Rev. B 31, 2957 (1985).

[20]M. Suzuki, Commun. Math. Phys. 57, 193 (1977).

[21]H. De Raedt, Comput. Phys. Rep. 7, 1 (1987).

[22]M. Barma and B. S. Shastry, Phys. Rev. B 18, 3351 (1978).

[23]P. De Vries, A. Lagendijk, and H. De Raedt, Phys. Rev. B 35, 5425 (1987).

[24]M. D. Feit, J. A. Fleck, Jr., and A. Steiger, J. Comput. Phys. 47, 412 (1982).

[25]W. Moffitt and W. Thorson, Phys. Rev. 108, 1251 (1957).

[26]M. D. Sturge, in Solid State Physics 20, edited by F. Seitz, D. Turnbull, and H. Ehrenreich (Academic, New York, 1967).

[27]F. S. Ham, Electron Paramagnetic Resonance (Plenum, New York, 1972).

[28]A. Abragam and B. Bleaney, Electron Paramagnetic Resonance of Transition Ions (Clarendon, Oxford, England, 1970).

[29]R. Englman, The Jahn-Teller Effect in Molecules and Crystals (Wiley-Interscience, New York, 1972).

[30]F. S. Ham, Phys. Rev. A 138, 1727 (1965).

[31]F. S. Ham, Phys. Rev. 166, 307 (1968).

[32]M. Caner and R. Englman, J. Chem. Phys. 44, 4054 (1966).

[33]U. Öpik and M. H. L. Pryce, Proc. R. Soc. London, Ser. A 238, 425 (1957).

[34]M. S. Child and H. C. Longuet-Higgins, Philos. Trans. R. Soc. London, Ser. A 254, 259 (1962).

[35]H. C. Longuet-Higgins, U. Öpik, M. H. L. Pryce, and R. Sack, Proc. R. Soc. London, Ser. A 244, 1 (1958).

[36]F. I. B. Williams, D. C. Krupka, and D. P. Breen, Phys. Rev. 179, 255 (1969).

[37]M. C. M. O'Brien, Proc. R. Soc. London, Ser. A 281, 323 (1964).

[38]J. R. Hoffman and T. L. Estle, Phys. Rev. B 27, 2640 (1983).

[39]N. Sakamoto, J. Phys. C 15, 6379 (1982).

[40]N. Sakamoto, Phys. Rev. B 31, 785 (1985).